

UC San Diego

UC San Diego Previously Published Works

Title

Titanium Surfaces Modified with Graphene Oxide/Gelatin Composite Coatings for Enhanced Antibacterial Properties and Biological Activities.

Permalink

<https://escholarship.org/uc/item/8dq351fr>

Journal

ACS Omega, 7(31)

Authors

Tan, Jing

Li, Lin

Li, Baoyuan

et al.

Publication Date

2022-08-09

DOI

10.1021/acsomega.2c02387

Copyright Information

This work is made available under the terms of a Creative Commons Attribution-NonCommercial-NoDerivatives License, available at <https://creativecommons.org/licenses/by-nc-nd/4.0/>

Peer reviewed

Titanium Surfaces Modified with Graphene Oxide/Gelatin Composite Coatings for Enhanced Antibacterial Properties and Biological Activities

Jing Tan, Lin Li, Baoyuan Li,* Xin Tian, Pengyuan Song, and Xueqi Wang



Cite This: *ACS Omega* 2022, 7, 27359–27368



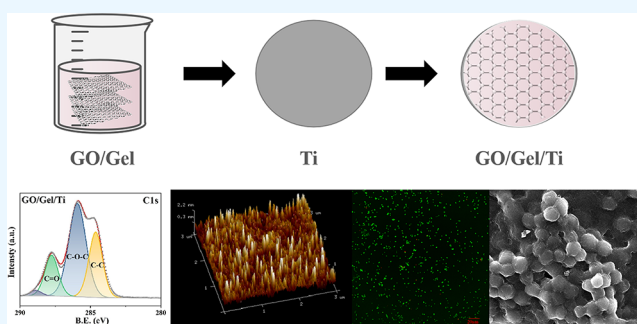
Read Online

ACCESS |

Metrics & More

Article Recommendations

ABSTRACT: Titanium alloys have been widely used in orthopedic implants due to their excellent physicochemical properties and good biocompatibility. However, in practice, titanium implants may fail to integrate or develop an implant-centered infection. Because of its excellent mechanical properties, bone integrability, biocompatibility, antibacterial properties, and so on, graphene oxide is increasingly being used in the preparation of composite biomaterials. The percutaneous titanium implants are used as the research object in this project. To solve the integration of implant and tissue, a graphene oxide/gelatin (GO/gel) composite coating was used to optimize the implant surface. Bacterial and cell experiments were used to investigate the antimicrobial activity, biocompatibility, and regulation of macrophage polarization of GO/gel-modified titanium. According to our findings, GO/gel-modified titanium has a good bacteriostatic effect against *Staphylococcus aureus*. On the modified surface, L929 cells proliferated well and showed no cytotoxicity. Simultaneously, the GO/gel-modified titanium surface could inhibit macrophage adhesion and spread in the early stage of culture and showed a more obvious inflammatory decline in the late stage of culture. These findings implied that GO/gel-modified titanium is advantageous for resistant bacteria and tissue remodeling.



1. INTRODUCTION

Because of their excellent mechanical properties and bone integration, titanium and its alloys have been widely used in percutaneous implants. The most significant issue limiting the clinical application of percutaneous implants is the interfacial reaction and bonding between the skin/subcutaneous tissue and implant.^{1,2} Titanium oxidizes easily in air, forming a TiO₂ film on the surface that is smooth, dense, and inert. The TiO₂ film on the surface of a titanium implant can form fibrous wrapping, preventing direct contact between the implant and tissue and resulting in poor osseointegration and soft tissue integration. As a result, we can use surface modification technology to improve the surface of titanium implants to improve their biological activity, bacteriostasis, and so on. The optimized surface improves the bonding strength between the implant and the soft tissue/bone tissue interface, increasing percutaneous implant success rates.^{3–5}

The researchers concentrate on two aspects to optimize the surface of the percutaneous implant. The first is to create bacteriostatic surfaces to prevent infection. Titanium has no bacteriostatic properties. We can directly create bacteriostatic surfaces by changing the surface morphology or adding antimicrobial agents,^{6–8} for example. We can also build an immune response surface to achieve bacteriostasis indirectly by

regulating immune cells to perform immune clearance.^{9,10} The other is creating a bioactive surface to aid in the integration of the implant and the host tissue. We can directly create bioactive surfaces by preparing porous surfaces or loading cytokines onto implant surfaces,^{11–13} for example. We can also build immune response surfaces to promote tissue integration between the implant and host by inducing macrophage phenotypic transformation indirectly.^{14,15}

Graphene oxide (GO) has been widely exploited in the production of composite biomaterials because of its superior mechanical characteristics, bone conductivity, bone inductivity, biocompatibility, antibacterial qualities, and ease of functionalization.^{16,17} GO acts as an antibacterial agent by disrupting the integrity of bacterial cell membranes.¹⁸ According to Lu's research, graphene's antibacterial function aids in wound healing.¹⁹ Hydrophilic GO can improve its contact with nearby cells and cell secretions and use its strong adsorption ability to

Received: April 16, 2022

Accepted: July 13, 2022

Published: July 25, 2022



adsorb certain protein molecules to its surface, affecting cell proliferation and differentiation.²⁰ The change of macrophages from M0 to M2 phenotypes has been demonstrated to be aided by GO.²¹ Xue's research has also shown that low concentrations of GO can activate macrophages to release vasculogenic and osteoblastic factors.²²

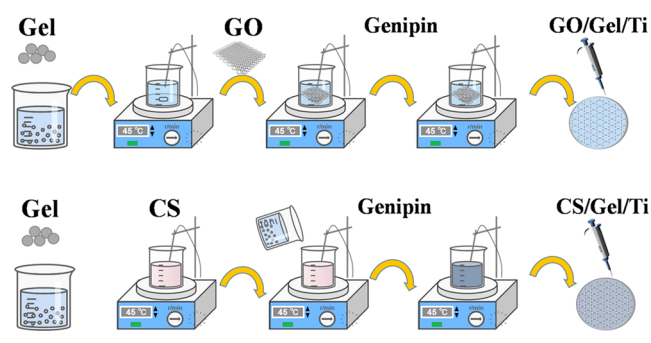
The use of graphene oxide in combination with other biomaterials can improve the surface qualities of materials, give them antibacterial capabilities, and control cell behavior. Gelatin is a polymer derived from collagen hydrolysis that is commonly used in the preparation of biomedical composites. Gelatin is biocompatible and degradable, and it can stimulate cell adhesion, proliferation, and stem cell differentiation. However, when used alone, gelatin has limitations, and studies have shown that using graphene as the reinforcing phase can significantly improve the mechanical properties of gelatin films.²³ Chitosan is biocompatible and has hemostasis, antibacterial, and wound healing properties. It is frequently combined with gelatin to make wound dressings to promote tissue repair.

In this study, we produced GO and gelatin (gel) composite coatings, as well as a chitosan/gelatin (CS/gel) composite coating for comparison, and employed these coatings to modify the surface of titanium implants. Antimicrobial activity, cell proliferation activity, and inflammatory factor release were all measured to see how bacteria and cells responded to GO/gel-modified titanium. To assess the potential of GO/gel-modified titanium for application, the antimicrobial, biocompatible, and immunomodulatory properties of GO/gel/Ti and CS/gel/Ti were combined and compared.

2. MATERIALS AND METHODS

2.1. Preparation of GO/Gel and CS/Gel Composite Membranes. Scheme 1 exhibits the fabrication process for

Scheme 1. Preparation of GO/Gel and CS/Gel-Modified Titanium



GO/gel and CS/gel-modified titanium. In brief, gelatin was the main component of composite membranes, and the antimicrobial and bioactive graphene and chitosan were added separately, with genipin acting as a cross-linking agent to prepare the GO/gel and CS/gel composite membranes separately. The preparation method is as follows. Gelatin solution with a concentration of 50 mg/mL was dissolved with stirring at 45 °C; then, 3% (v/v) glycerol was added and stirred for 30 min in a water bath at 45 °C, followed by 5% (v/v) GO solution with a concentration of 5 mg/mL and continuous stirring and comixing to produce a mixed GO/gel film-forming solution. Ultrasonication was used to dissolve genipin in a 60% ethanol solution, yielding a 5% (w/v) genipin solution. GO/

gel-1 and GO/gel-2 are two types of composite membranes that contain 0.2 and 2% (w/w) of genipin, respectively. The CS/gel membrane solution contains 0.8% (w/v) gelatin and 0.8% (w/v) chitosan, and CS/gel composite membranes with varying degrees of cross-linking were created by adding 0.2 and 2% genipin. The composite membranes were given the names CS/gel-1 and CS/gel-2. The film solution is cast into the poly(vinyl chloride) (PVC) board to form a film, which is then cut to the appropriate size for testing after drying.

2.2. Characterization of Composite Membranes. A scanning electron microscope was used to examine the surface topography of the composite membranes (SEM, Inspect, FEI). A thermal analyzer (TGA/DSC 3+, METTLER TOLEDO) was used for the thermogravimetric analysis (TGA). The swelling behavior of composite membranes in phosphate buffer saline (PBS) at 37 °C was studied using a gravimetric method. In brief, composite membranes of known weight (W1) were swollen in PBS first. The composite membranes were removed from the PBS at predetermined time intervals, and the hydrated membrane weight (W2) was measured after removing excess liquid from the surface with wet filter paper. This procedure was repeated several times until a swelling equilibrium was reached. The swelling ratio (SR) was calculated as follows.

$$SR = \frac{W2 - W1}{W1} \times 100\%$$

2.3. Release Kinetics of Composite Membranes. To test the release kinetics of the composite membranes, bovine serum albumin (BSA) was chosen as the model protein. BSA solution (1 mg/mL) was added to the composite membrane solution, and then the genipin was added to make the composite membrane. The membrane was cut into 3 cm × 3 cm squares and placed in a centrifuge tube with 50 mL of PBS. At 25 °C and 150 rpm, the sample was oscillated. Two hundred microliters of release solution were extracted at predetermined time intervals and stored at −18 °C until measured. The modified BCA Protein Assay Kit (Sangon Biotech) was used to determine the BSA content of the release solution.

2.4. Preparation and Characterization of GO/Gel-Modified Titanium (GO/Gel/Ti). Titanium sheets were pretreated using the same method as in our previous study.²⁴ A compound membrane solution containing 2% genipin was prepared, and GO/gel and CS/gel-modified titanium (CS/gel/Ti) were created by sprinkling the film droplets onto the titanium sheet and drying at 37 °C.

Surface roughness and morphology were measured using atomic force microscopy (AFM; Dimension Icon, Bruker). A contact angle instrument (DSA30, Kruss, Germany) was used to evaluate the hydrophilic–hydrophobic properties of samples, and photographs were taken. The surface chemical compositions of samples were determined by X-ray photoelectron spectroscopy (XPS) (K-α+, Thermo Scientific) through full XPS spectra and detailed spectra of C 1s/O 1s peaks. Fourier transform infrared (FTIR) spectra of samples were recorded using a Thermo Fisher Nicolet IS- 50 spectrometer in the 4000–500 cm^{−1} range.

2.5. In Vitro Antibacterial Tests. *Staphylococcus aureus*, a common species in infections, was used to evaluate the antibacterial ability of GO/gel/Ti and CS/gel/Ti in vitro; pure titanium (Ti) samples were set as control. *S. aureus* (ATCC 29213) was cultured in the LB medium and prepared at

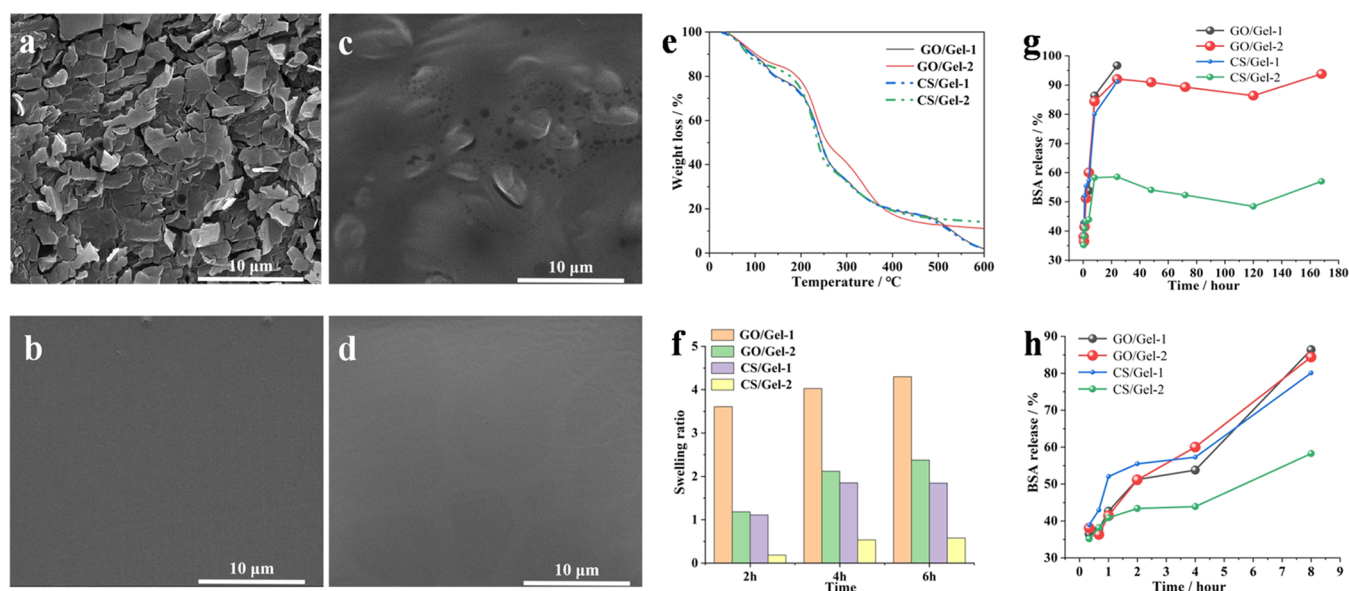


Figure 1. Characterization of the GO/gel and CS/gel composite membranes: (a–d) SEM images showing the surface topography of GO/gel-1 (a), GO/gel-2 (b), CS/gel-1 (c), and CS/gel-2 (d) at 10 k magnification; (e) TGA curve of GO/gel-1, GO/gel-2, CS/gel-1, and CS/gel-2; (f) swelling ratio of GO/gel-1, GO/gel-2, CS/gel-1, and CS/gel-2; and (g, h) release kinetic curve of GO/gel-1, GO/gel-2, CS/gel-1, and CS/gel-2 in 168 h (g) and 8 h (h).

concentrations of approximately 1.0×10^6 CFU/mL. For the antibacterial experiment, samples were placed in a 24-well plate after sterilizing with UV light, and 1 mL of bacterial suspension was added to the surfaces of the samples. The samples were then cultured at 37 °C for 4 and 24 h. The samples were rinsed to remove nonadherent bacteria and vigorously shaken to transfer bacteria from the sample surface to the liquid. The bacterial solution was diluted, and the suspension was spread on a nutrient agar plate and incubated for counting. The antibacterial rate was calculated using these observations. Laser scanning confocal microscopy (LSCM) was used to assess the states of *S. aureus*. The sample was cultured for 4 h at 37 °C and rinsed to remove floating bacteria. The bacteria on the samples were stained for 15 min in a staining working solution (1 mL PBS solution containing 1 μ L SYTO 9 and 1 μ L PI). LSCM (FV1200, Olympus) was conducted to observe and capture images of live and dead bacteria.

2.6. Cytocompatibility Evaluation of the Samples.

L929 cells were seeded on GO/gel/Ti and CS/gel/Ti surfaces, and cytotoxicity was assessed using the MTT assay. The samples were placed in 24-well plates at 1.0×10^5 cells/mL cell density. Cells incubated in the absence of samples served as a control. At predetermined time periods, the medium was removed and samples were rinsed twice with PBS. Each well received a 300 μ L volume of MTT medium. After 4 h, the supernatant was removed, 300 μ L of dimethylsulfoxide (DMSO) was added per hole, and the table was shaken for 10 min to fully dissolve the crystals. The medium (200 μ L) was transferred to a 96-well plate, and the absorbance was measured at 570 nm. SEM was used to examine the morphology of cells on the samples. Samples were taken at each time point, washed twice in PBS to remove unattached cells, and fixed with a 2.5% glutaraldehyde solution.

2.7. Macrophage Responses to GO/Gel/Ti and CS/Gel/Ti. The biological behavior of macrophages was investigated using RAW264.7 cells. The cells were mechanically isolated, and the cell suspension concentration was

adjusted to a density of 5×10^4 cells/mL. After that, the cells were reseeded on sample surfaces in 24-well cell culture plates. After 1, 3, and 7 days of culture, cell proliferation was measured using the MTT assay, and cell morphology was studied under SEM. The cell culture supernatant was collected at each time point to assess the cytokine release produced by the activated macrophages adhering to the samples. Enzyme-linked immunosorbent assay (ELISA) kits were used to evaluate the release of cytokines (TNF- α , IL-6, and IL-10).

2.8. Statistical Analysis. All of the assays were repeated three times in a random order. The information is presented in the form of a mean and standard deviation (SD). The in vivo and in vitro experimental results were statistically analyzed using one-way analysis of variance (ANOVA), with a *p* value of 0.05 regarded statistically significant.

3. RESULTS AND DISCUSSION

3.1. Characterization of the GO/Gel and CS/Gel Composite Membranes. The surface topography of the samples was observed by SEM (Figure 1a–d). When the content of genipin was 0.2%, SEM images revealed irregular micron-sized pits on the GO/gel surfaces (Figure 1a), which are characteristic nanosized wrinkle-like structures of GO known as asperities. When the content of genipin was increased to 2%, the smooth surface of the GO/gel-2 samples was observed (Figure 1b). The surface of the CS/gel composite film is uneven and bulging when the genipin concentration is 0.2% (Figure 1c), which could be due to chitosan particle aggregation, whereas when the genipin concentration is increased to 2%, the surface is compact and smooth (Figure 1d). Genipin contains hydroxyl and carboxyl groups, which can react with the amino groups in gelatin and chitosan to form a polymer network structure. Because of these intermolecular or intramolecular cross-links, the GO/gel-2 and CS/gel-2 composite membranes have a compact and smooth surface structure.

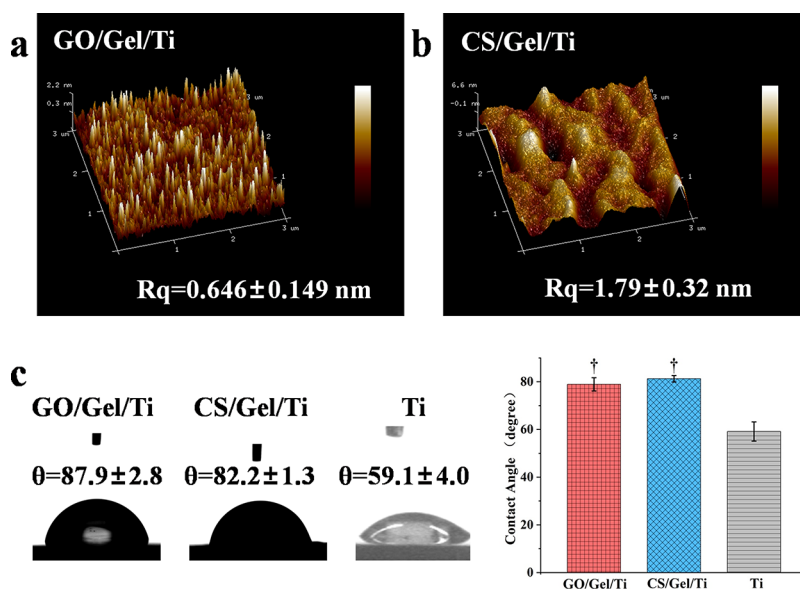


Figure 2. Surface characterization of the GO/gel/Ti and CS/gel/Ti samples: (a, b) three-dimensional surface microstructures of the samples were detected by AFM; (c) contact angle measurements showing the hydrophilicity and hydrophobicity of the samples, $\dagger p < 0.05$ compared to the Ti sample.

The thermal properties of GO/gel-1, GO/gel-2, CS/gel-1, and CS/gel-2 were investigated by TGA (Figure 1e). The TGA curves of all samples show similar trends, and the composite film shows two distinct stages of weight loss. The first stage is from 25 to 200 °C; the weight loss in this stage is mainly caused by the evaporation of water in the composite film. The second stage occurring at 200–400 °C was attributed to the decomposition of the composite film. Comparing the composite membranes with different degrees of cross-linking, the residual masses of GO/gel-1 and GO/gel-2 were 2.11 and 11.06%, respectively. For CS/gel-1 and CS/gel-2, the residual masses were 2.23 and 13.85%, respectively. Strong inter- and intramolecular interactions were generated between the reactive groups in the genipin molecule and the reactive groups on the gelatin and chitosan molecules, and the polymer network structure formed as the genipin content increased was more compact, resulting in a higher residual mass of the GO/gel-2 and CS/gel-2.

Figure 1f depicts the swelling characteristics of GO/gel-1, GO/gel-2, CS/gel-1, and CS/gel-2. All of the composite membranes gradually absorbed water and reached equilibrium by the end of the measurement (6 h). When comparing the composite membranes with the same genipin content, the swelling rate of GO/gel is higher than CS/gel, which is owing to the high gelatin content in GO/gel for the two composite membranes of the same grade. Gelatin contains many hydrophilic polar groups that can interact with water molecules and induce them to enter the network structure of the membrane, causing the membrane to swell, and the swelling of the membrane facilitates bacterial inhibitors to migrate to the surrounding media. Furthermore, as the genipin content increased from 0.2 to 2.0%, the swelling rate of the composite membrane decreased significantly. Cross-linking with genipin can significantly reduce the swelling rate of membrane materials, making it an effective method of loading drugs for slow release.

Figure 1g,f demonstrates the release kinetic curves of GO/gel and CS/gel composite membranes with varying degrees of

cross-linking in a PBS buffer. The release of BSA from composite membranes was divided into three stages: explosive (0–8 h), slow (8–24 h), and finally reaching release equilibrium (1–7 days). In the first 1 h, the release rate of BSA in all samples was greater than 40%. When the genipin content was low, the release rate was close to 90% in 8 h, and the GO/gel-1 and CS/gel-1 samples had been completely decomposed in the buffer system at this time. When the genipin content increased to 2%, the release rates for GO/gel-2 and CS/gel-2 were about 85 and 58% in 8 h, respectively. The release rate of CS/gel-2 was significantly lower than CS/gel-1. After 8 h, the release rate was barely increasing, and the composite membranes immersed in the buffer system retained their structure. The network structure of the composite membrane became more compact as the cross-linking agent dosage was increased. Genipin interacts more closely with gelatin and chitosan molecules, resulting in more controlled and slow release. This corresponds to the swelling characteristic.

The above results indicated that as the amount of genipin increased, the surface morphology of the composite membranes flattened, the swelling rate decreased, the thermal stability improved, and the ability to control the release of the contained drug enhanced. As a result, a composite membrane system containing 2% genipin was chosen for the surface modification of titanium implants.

3.2. Surface Characterization of the GO/Gel/Ti and CS/Gel/Ti Surfaces. The three-dimensional surface microstructures of the samples are shown in Figure 2a,b. A lattice structure was observed on the GO/gel/Ti sample, while a similar structure was not observed on the CS/gel/Ti surface. For GO/gel/Ti, the root mean square of the Z data (Rq) was 0.646 ± 0.149 nm, indicating a smoother surface than the surface with the CS/gel coating (the Rq was 1.79 ± 0.32 nm). The contact angle (CA) indicates the hydrophilicity or hydrophobicity of the sample surfaces. Figure 2c shows the CAs of GO/gel/Ti, CS/gel/Ti, and Ti, which were $87.9^\circ \pm 2.8$, $82.2^\circ \pm 1.3$, and $59.1^\circ \pm 4.0$, respectively, indicating that

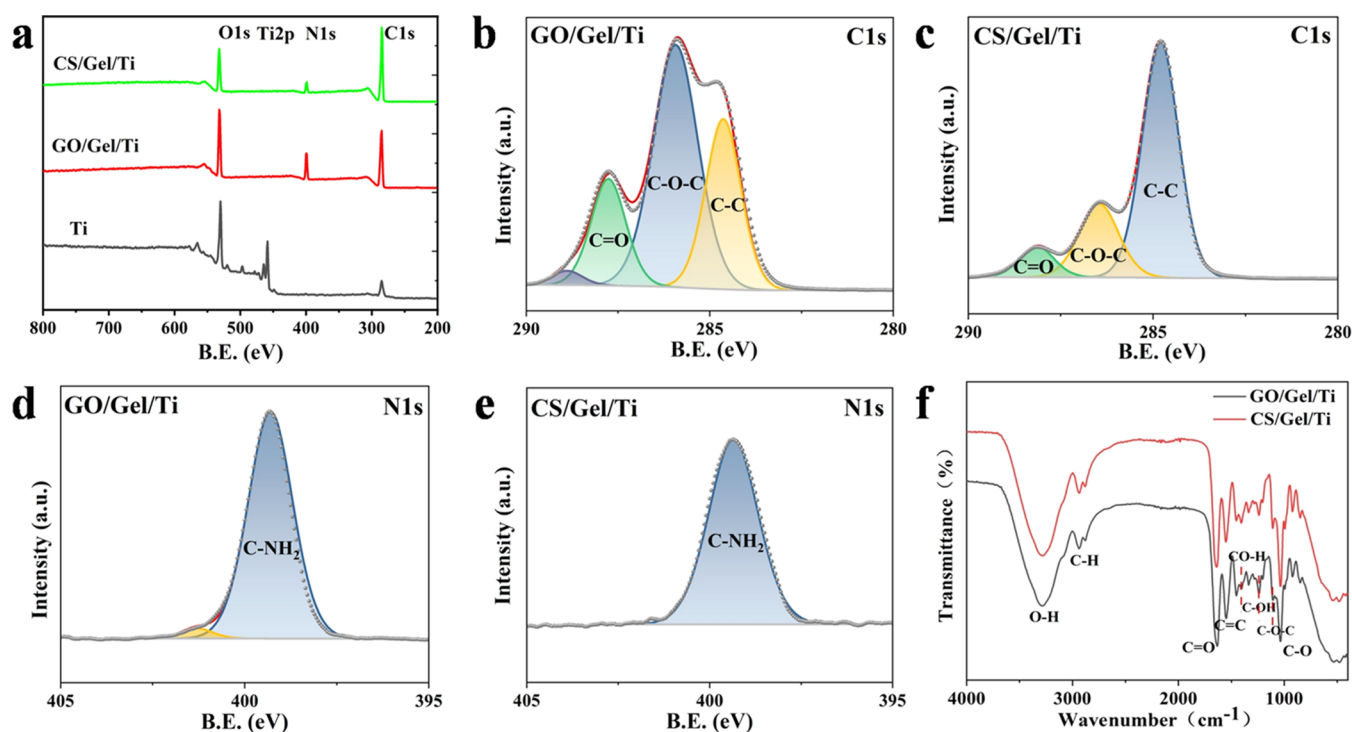


Figure 3. XPS and FTIR spectrum of the samples: (a) XPS full spectrum; (b, c) resolved peaks of C 1s spectra on GO/gel/Ti and CS/gel/Ti surfaces; (d, e) resolved peaks of N 1s spectra on GO/gel/Ti and CS/gel/Ti surfaces; and (f) FTIR spectrum of the samples.

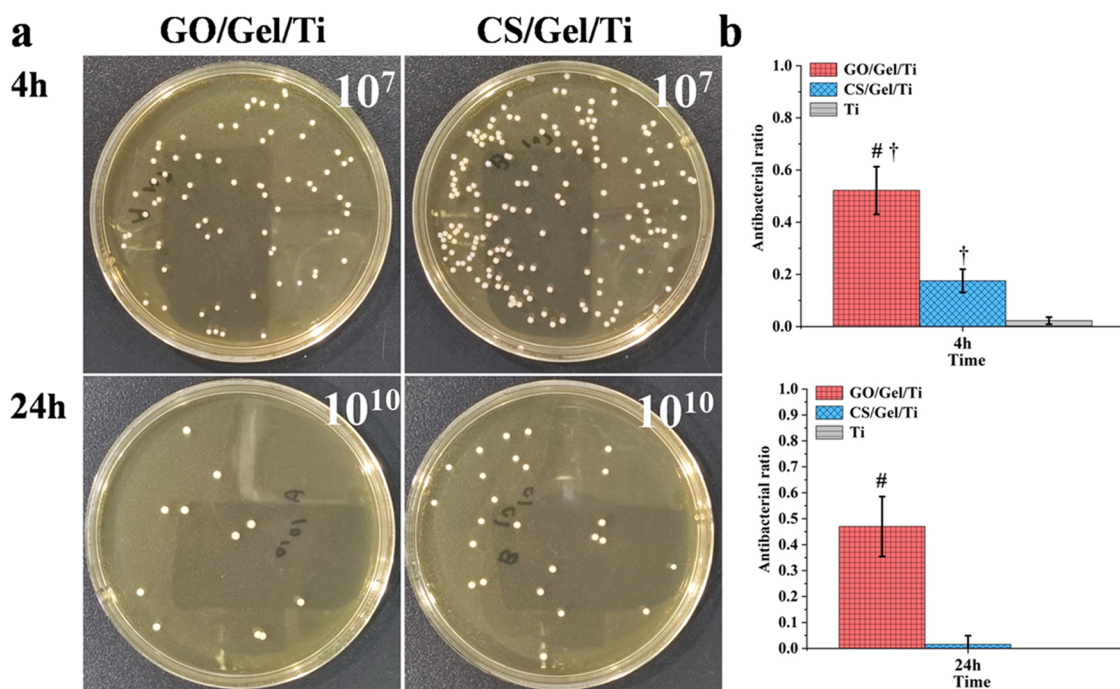


Figure 4. Antibacterial property of the GO/gel/Ti and CS/gel/Ti samples. (a) Representative images of *S. aureus* colony-forming units for GO/gel/Ti and CS/gel/Ti. (b) Results of antibacterial rates. # $p < 0.05$ compared to the CS/gel/Ti sample and † $p < 0.05$ compared to the Ti sample.

all samples were hydrophilic. This characteristic is important for protein adsorption and cell attachment of the material surface.

XPS analysis revealed significant differences in the chemical composition of GO/gel/Ti and CS/gel/Ti. Full spectra of the samples are shown in Figure 3a. The N 1s peaks appeared on the surface of GO/gel/Ti and CS/gel/Ti, and the Ti 2p regions disappeared. To establish a better understanding of

chemical components, XPS C 1s peak fitting was performed. As shown in Figure 3b, there were three C 1s peaks with GO/gel/Ti, which could be attributed to C–C at 284.6 eV, C–O–C at 285.9 eV, and C=O at 287.6 eV. The introduction of GO shifted it into a higher binding energy domain, with two main peaks consisting of C–O–C and C=O. There was only one main C 1s peak with CS/gel/Ti in Figure 3c, which could be

attributed to C–C at 284.8 eV. N 1s spectra of GO/gel/Ti and CS/gel/Ti (Figure 3d,e) were attributed to –NH₂ at 399.3 eV.

The chemical structures of the samples were characterized by Fourier transform infrared (FTIR) spectroscopy (Figure 3f). For GO/gel/Ti, characteristic peaks at 3300, 1700, 1600, and 1100 cm⁻¹ could be attributed to –OH, C=O, C=C, and C–O–C stretchings, respectively. These characteristic absorptions proved the existence of oxygen-containing groups such as carboxyl, hydroxyl, and epoxy groups in graphene oxide, and the relative intensities between the vibrational peaks did not change significantly in comparison with the GO infrared spectrum. These indicated that the incorporation of GO into the gelatin system did not undergo chemical changes, but the GO existed in the composite in the form of physical dispersion. For CS/gel/Ti, characteristic peaks at 3300, 1600, 1400, and 1100 cm⁻¹ could be attributed to –NH₂, NH, C–H, and C–O–C stretchings, respectively. After blending chitosan and gelatin, the protonated amino group in CS reacted with –COO– in gel, while the amino groups in both chitosan and gelatin molecules cross-linked with genipin to form a polymer network, resulting in the red shift of the –OH and NH stretching vibrational convergence peaks in the surface.

3.3. In Vitro Antimicrobial Activity of the GO/Gel/Ti and CS/Gel/Ti. The antibacterial properties of GO/gel/Ti and CS/gel/Ti against *S. aureus* were investigated. The amount of bacteria on the surface of CS/gel-modified titanium was significantly greater than that of GO/gel/Ti, as indicated by the representative images in Figure 4a, and both groups of samples did not show a very significant bacterial inhibition effect, and the number of colonies still increased significantly at 24 h when compared with the 4 h count results. Figure 4b shows that for antibacterial activities, pure Ti was used as the control group. The bacteria grew rapidly in the Ti group, while bacterial quantity decreased significantly in the GO/gel/Ti group. When comparing the two composite membrane-modified titanium, graphene oxide clearly outperforms the other in terms of improving the antibacterial performance of titanium implants.

Fluorescence staining of bacteria was used to confirm the antibacterial effect of the samples. Live bacteria were labeled with SYTO 9 (a nucleic acid stain) to produce green fluorescence, and dead bacteria were labeled with PI (which shows red fluorescence, owing to the destruction of the cell membrane). The results are similar to the spread plate images. As shown in Figure 5, the control Ti group showed almost all green fluorescence, and the number of live bacteria was much higher than that in GO/gel/Ti and CS/gel/Ti groups. By contrast, in the GO/gel/Ti, the green fluorescence was significantly weakened and the red fluorescence was enhanced, suggesting that GO could effectively rupture cytoplasmic membranes and induce the death of bacteria. GO as a nanomaterial plays the role of nanoknife directly affecting the cell membrane. The bacteria can be chemically destroyed by GO because the GO surface contains some chemical functional groups. They can combine with protease in bacterial cell membranes, extracting phospholipids and other substances from the cell membrane and causing its shrinkage and deformation.²⁵

The antibacterial effect of chitosan has been demonstrated to be due to the interaction of the positive charge carried by its molecules with the negative charge carried by the microbial cell membrane, resulting in the leakage of proteins and other cellular components of bacteria.²⁶ The failure of CS/gel/Ti to

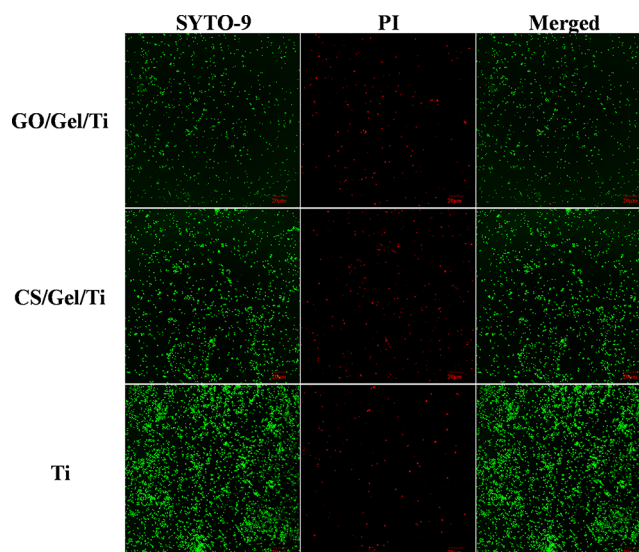


Figure 5. Stained images of live (green fluorescence) and dead (red fluorescence) *S. aureus* distributed on the GO/gel/Ti, CS/gel/Ti, and Ti samples.

exert an antibacterial effect may be due to the reaction between the –NH₂ group in the molecular chain of chitosan and genipin after the cross-linking reaction between these two. It has been demonstrated that chitosan has an antibacterial effect under weakly acidic conditions when the –NH₂ protonation in its molecular chain is transformed to –NH³⁺, but it does not have antibacterial properties when the pH value is high because the –NH³⁺ is transformed into –NH₂.²⁷

These findings are consistent with the XPS and FTIR data (Figure 3). GO was present in the composite coating in a physically dispersed manner in the GO/gel/Ti, and the antibacterial effect was effective. For CS/gel/Ti, the antibacterial component of chitosan exists in the –NH₂ form, rendering it ineffective against bacteria. All of these findings support the bacteriostaticity of GO/gel/Ti, demonstrating the potential to prevent bacterial infections.

3.4. In Vitro Biocompatibility of the GO/Gel/Ti and CS/Gel/Ti. The cell compatibility of the GO/gel/Ti and CS/gel/Ti was investigated using a direct contact assay between the modified titanium and mouse-derived fibroblasts (L929). There was good cell proliferation activity after 1 and 3 days of cocultivation. At 7 days, the proliferative activity of cells in all groups decreased significantly. These results indicated that the modified titanium surface was not cytotoxic (Figure 6a). Furthermore, the SEM assay was used to assess the cell compatibility of the GO/gel/Ti and CS/gel/Ti. As shown in Figure 6b, cells on the CS/gel/Ti surface spread well, as evidenced by the cell-to-cell interconnection via protruding pseudopods, whereas cells on the GO/gel/Ti surface spread less well, with fewer protruding pseudopods and less cell-to-cell connection. In addition, previous studies reported that a GO dose less than 125 mg/kg does not cause toxicity²⁸ and GO in the appropriate concentration range can improve the biological activity of composites.^{29,30} Overall, the GO/gel modification had no toxic effect on cell survival and good biocompatibility.

3.5. Macrophage Responses of the GO/Gel/Ti and CS/Gel/Ti. RAW264.7 cells were cultured on the GO/gel/Ti and CS/gel/Ti to observe morphology, proliferation, and cytokine secretion to assess the contribution of macrophages to anti-infection and tissue repair. SEM was used to examine the

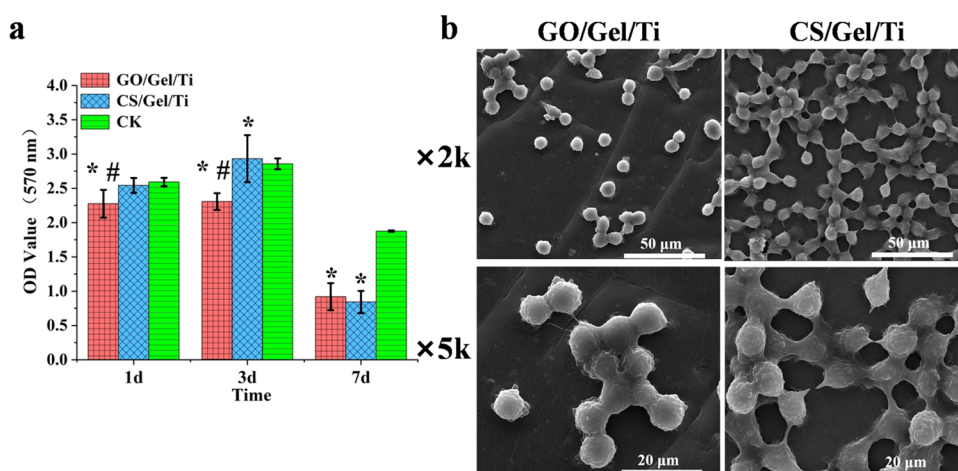


Figure 6. Biocompatibility evaluation of GO/gel/Ti and CS/gel/Ti. (a) Cell viability of indicated groups coincubated with L929 cells for 1, 3, and 7 days ($n = 3$). (b) SEM images of L929 cells after contact with samples for 3 days. * $p < 0.05$ compared to the cell control (CK) and # $p < 0.05$ compared to the CS/gel/Ti sample.

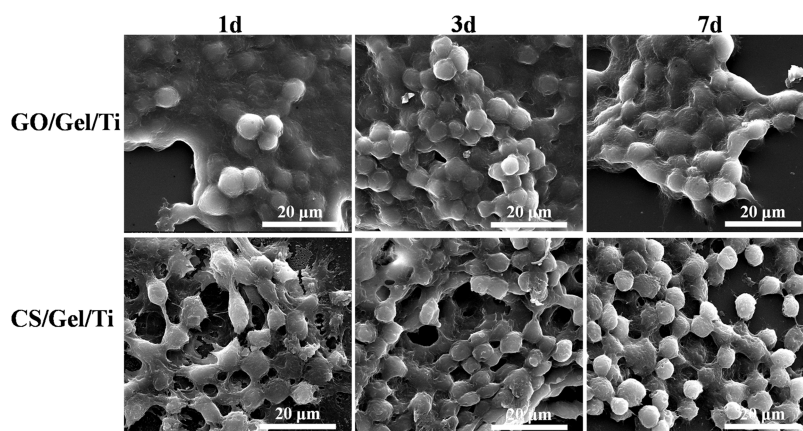


Figure 7. SEM images of macrophages cultured on GO/gel/Ti and CS/gel/Ti surfaces at 1, 3, and 7 days.

morphology of macrophages after 1, 3, and 7 days of culture on samples (Figure 7). The majority of the macrophages on the GO/gel/Ti surface remained round, with smooth edges and abundant matrix secretion. At day 1, the macrophages on CS/Gel/Ti were well extended and had several pseudopods protruding, but as the culture time was extended, the cell morphology retracted, the cell morphology wrinkled, and the pseudopods were reduced. This indicated that the GO/gel-modified titanium surface does not promote macrophage migration and spreading, and the cells on this surface are round, whereas the CS/gel/Ti activated macrophage migration at the start of the culture, exhibiting pseudopod protrusion and cell spreading.

Figure 8a depicts the macrophage cell proliferation after 1, 3, and 7 days of culture on samples. After 1 day of culture, there was no significant difference in the cell proliferation activity of each group, and as culture time was extended, the cell viability all increased by a certain amount, but the increase of the CS/gel/Ti samples was not as obvious as the other two groups. This implied that the proliferation of macrophages on the surface of GO/gel/Ti was the best, and cell activity was comparable to that of the pure cell control, whereas the promotion of macrophage proliferation on the surface of CS/gel/Ti was insignificant.

Activated macrophages further secrete cytokines to regulate the immune response and tissue regeneration. Then, we investigated the effects of different surfaces on cytokine secretion by macrophages. As shown in Figure 8b–d, the CS/gel/Ti surface promoted inflammatory factor $\text{TNF-}\alpha$, IL-6, and IL-10 secretions, while the GO/gel/Ti surface inhibited the secretion of these three cytokines above compared with the CS/gel/Ti surface. There was also no significant difference in $\text{TNF-}\alpha$ and IL-6 secretions between GO/gel/Ti and the pure cell control group, but IL-10 secretion was higher on the GO/gel/Ti surface than that on the pure cell control in the early stages of culture. Increased IL-10 secretion allows macrophages to adopt a phenotype that suppresses inflammation and promotes tissue repair. It has been shown that a small amount of graphene oxide can promote the conversion of macrophages from M0 to M2 type.²¹ Furthermore, cytokine secretion in the three groups decreased with increasing time, indicating that the inflammation was gradually alleviated. The secretion of these cytokines is consistent with the morphology of macrophage on different surfaces.

Based on the above results (Figures 7 and 8), it has been confirmed that different material surface characteristics have various effects on the responses of macrophages. In the initial stages of culture, there was little difference in the proliferation activity of the cells in each group, and there was more matrix

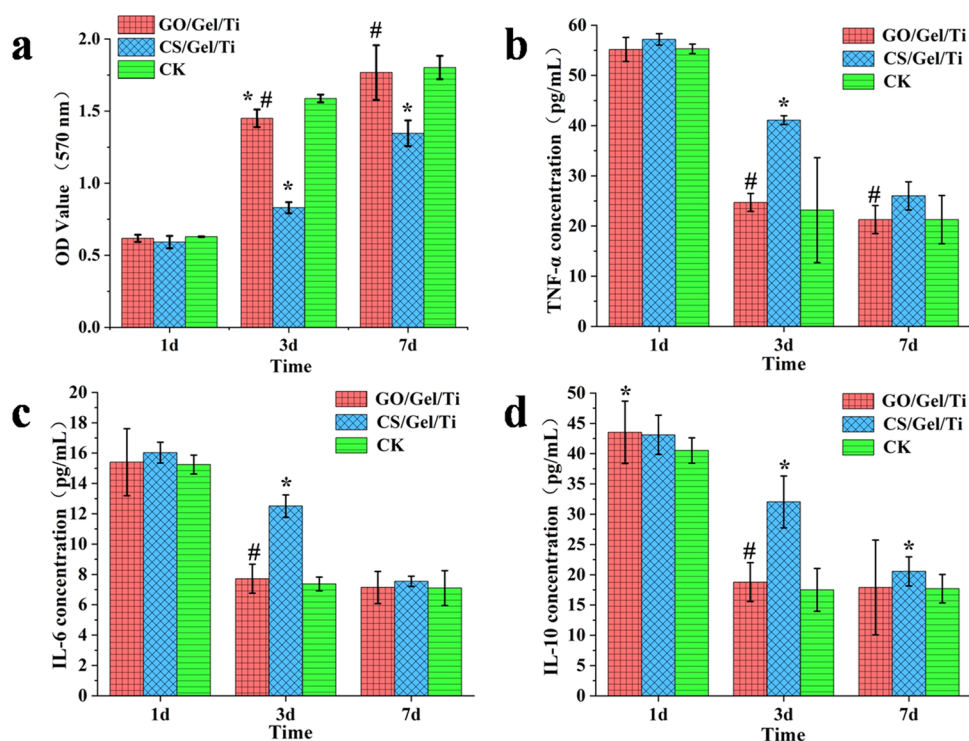


Figure 8. (a) Cell proliferation of macrophages cultured on GO/gel/Ti and CS/gel/Ti surfaces at 1, 3, and 7 days. (b–d) Cytokine secretion from macrophages on GO/gel/Ti and CS/gel/Ti surfaces was analyzed by ELISA at 1, 3, and 7 days. (b) TNF- α , (c) IL-6, and (d) IL-10. * $p < 0.05$ compared to the cell control (CK) and # $p < 0.05$ compared to the CS/gel/Ti sample.

secretion on the surface of GO/gel-modified titanium, which was beneficial to subsequent cell proliferation. Furthermore, the presence of GO limited cell spreading and inhibited the secretion of inflammatory factors. The CS/gel-modified titanium group had better cell spreading than the GO group, indicating that this surface activated macrophages to M1-type polarization and the cells secreted more inflammatory factors. The cells on the surface of CS/gel/Ti began to retract, and the pseudopods were reduced at the late stage of culture, and the inflammatory response of macrophages in all groups was downregulated at this time. Pure macrophages are more proliferative in culture than that on modified materials, and both activation and recession of the inflammatory response can be insignificant.

GO and chitosan are frequently used as antimicrobial agents to modify the surface of implant materials. While GO has excellent antimicrobial properties, its biocompatibility is greatly affected by concentration, whereas chitosan is biocompatible but has limited antimicrobial activity. We compared the antibacterial properties and biocompatibility of GO/gel-modified titanium to CS/gel/Ti. In this study, the XPS and FTIR results showed that GO in the composite coating did not undergo chemical changes; the antibacterial effect of GO/gel/Ti was greater than that of CS/gel/Ti. Both groups of modified titanium have good wettability and surface roughness, and the cells proliferated well on the surfaces of the materials. Numerous studies have demonstrated that hydrophilic material surfaces reduce macrophage adhesion and inflammatory activity.³¹ Simultaneously, GO can inhibit inflammatory responses and promote wound healing and angiogenesis by modulating macrophage phenotypic transition.³² Thus, macrophages cultured on the GO/gel/Ti surface created an anti-

inflammatory environment, which is beneficial for improving the healing of biomaterials.

4. CONCLUSIONS

In the present study, we first prepared GO/gel and CS/gel composite films with varying degrees of cross-linking and characterized their properties such as microscopic morphology, swelling rate, thermal weight, and release kinetics. The composite membrane with a genipin content of 2% had excellent material properties and was thus chosen for the indicated titanium modification. Then, we examined the surface characterization, antibacterial properties, and biocompatibility of GO/gel-modified titanium, compared with those of CS/gel/Ti. GO/gel-modified titanium has good hydrophilicity and lower surface roughness, and GO existed in the coating in the form of physical dispersion. The GO/gel/Ti exhibited stronger antibacterial properties against *S. aureus*, and it did not have adverse effects on the growth of L929 cells. However, the GO/gel/Ti surface can limit the spreading of macrophages and stronger inflammatory response. Therefore, this study presents a feasible method for the surface modification of GO/gel coating on titanium to obtain enhanced antibacterial activity and biocompatibility.

Low doses of GO have been shown to stimulate macrophages to secrete angiogenic and osteogenic cytokines,²² implying that GO can regulate bone regeneration via the immune microenvironment.³³ As a result, our next study should look into the effect of GO/gel-modified titanium on macrophage phenotypic transformation and the secretion of related osteogenic and angiogenic factors, as well as the effect of GO/gel/Ti on MSC osteogenic differentiation and endothelial cell angiogenesis. To find the best GO/gel composite membrane preparation for bone, we must also

further investigate the gradient–effect relationship between GO dose and related cell behavior in composite membranes.

AUTHOR INFORMATION

Corresponding Author

Baoyuan Li – School of Life Science, Shanxi Datong University, Datong 037009 Shanxi, China; Institute of Applied Biotechnology, Shanxi Datong University, Datong 037009 Shanxi, China; orcid.org/0000-0003-3895-1154; Email: liby616@163.com

Authors

Jing Tan – School of Life Science, Shanxi Datong University, Datong 037009 Shanxi, China; Institute of Applied Biotechnology, Shanxi Datong University, Datong 037009 Shanxi, China

Lin Li – Shanxi Datong University, Datong 037009 Shanxi, China

Xin Tian – School of Life Science, Shanxi Datong University, Datong 037009 Shanxi, China

Pengyuan Song – School of Life Science, Shanxi Datong University, Datong 037009 Shanxi, China

Xueqi Wang – School of Life Science, Shanxi Datong University, Datong 037009 Shanxi, China

Complete contact information is available at:

<https://pubs.acs.org/10.1021/acsomega.2c02387>

Notes

The authors declare no competing financial interest.

ACKNOWLEDGMENTS

This work was supported by the Applied Basic Research Project of Shanxi Province (201801D221097).

REFERENCES

- (1) Abdallah, M.-N.; Badran, Z.; Ciobanu, O.; Hamdan, N.; Tamimi, F. Strategies for Optimizing the Soft Tissue Seal around Osseointegrated Implants. *Adv. Healthcare Mater.* **2017**, *6*, No. 1700549.
- (2) Thesleff, A.; Brånemark, R.; Håkansson, B.; Ortiz-Catalan, M. Biomechanical Characterisation of Bone-Anchored Implant Systems for Amputation Limb Prostheses: A Systematic Review. *Ann. Biomed. Eng.* **2018**, *46*, 377–391.
- (3) Wang, Y.; Zhang, Y.; Miron, R. J. Health, Maintenance, and Recovery of Soft Tissues around Implants: Soft Tissues around Implants. *Clin. Implant Dent. Res.* **2016**, *18*, 618–634.
- (4) Shao, J.; Kolwijck, E.; Jansen, J. A.; Yang, F.; Walboomers, X. F. Animal Models for Percutaneous-Device-Related Infections: A Review. *Int. J. Antimicrob. Agents* **2017**, *49*, 659–667.
- (5) Kaur, M.; Singh, K. Review on Titanium and Titanium Based Alloys as Biomaterials for Orthopaedic Applications. *Mater. Sci. Eng., C* **2019**, *102*, 844–862.
- (6) Chourifa, H.; Bouloussa, H.; Migonney, V.; Falentin-Daudré, C. Review of Titanium Surface Modification Techniques and Coatings for Antibacterial Applications. *Acta Biomater.* **2019**, *83*, 37–54.
- (7) Yin, I. X.; Zhang, J.; Zhao, I. S.; Mei, M. L.; Li, Q.; Chu, C. H. The Antibacterial Mechanism of Silver Nanoparticles and Its Application in Dentistry. *Int. J. Nanomed.* **2020**, *15*, 2555–2562.
- (8) Tang, G.; He, J.; Liu, J.; Yan, X.; Fan, K. Nanozyme for tumor therapy: Surface modification matters. *Exploration* **2021**, *1*, 75–89.
- (9) Tan, J.; Zhao, C.; Wang, Y.; Li, Y.; Duan, K.; Wang, J.; Weng, J.; Feng, B. Nano-Topographic Titanium Modulates Macrophage Response in Vitro and in an Implant-Associated Rat Infection Model. *RSC Adv.* **2016**, *6*, 111919–111927.
- (10) He, Y.; Li, K.; Yang, X.; Leng, J.; Xu, K.; Yuan, Z.; Lin, C.; Tao, B.; Li, X.; Hu, J.; Dai, L.; Becker, R.; Huang, T. J.; Cai, K. Calcium Peroxide Nanoparticles-Embedded Coatings on Anti-Inflammatory TiO₂ Nanotubes for Bacteria Elimination and Inflammatory Environment Amelioration. *Small* **2021**, *17*, No. 2102907.
- (11) Souza, J. C. M.; Sordi, M. B.; Kanazawa, M.; Ravindran, S.; Henriques, B.; Silva, F. S.; Aparicio, C.; Cooper, L. F. Nano-Scale Modification of Titanium Implant Surfaces to Enhance Osseointegration. *Acta Biomater.* **2019**, *94*, 112–131.
- (12) Arcos, D.; Vallet-Regí, M. Substituted Hydroxyapatite Coatings of Bone Implants. *J. Mater. Chem. B* **2020**, *8*, 1781–1800.
- (13) Tao, F.; Ma, S.; Tao, H.; Jin, L.; Luo, Y.; Zheng, J.; Xiang, W.; Deng, H. Chitosan-Based Drug Delivery Systems: From Synthesis Strategy to Osteomyelitis Treatment - A Review. *Carbohydr. Polym.* **2021**, *251*, No. 117063.
- (14) Luu, T. U.; Gott, S. C.; Woo, B. W. K.; Rao, M. P.; Liu, W. F. Micro- and Nanopatterned Topographical Cues for Regulating Macrophage Cell Shape and Phenotype. *ACS Appl. Mater. Interfaces* **2015**, *7*, 28665–28672.
- (15) Hotchkiss, K. M.; Reddy, G. B.; Hyzy, S. L.; Schwartz, Z.; Boyan, B. D.; Olivares-Navarrete, R. Titanium Surface Characteristics, Including Topography and Wettability, Alter Macrophage Activation. *Acta Biomater.* **2016**, *31*, 425–434.
- (16) Guo, C.; Lu, R.; Wang, X.; Chen, S. Graphene Oxide-Modified Polyetheretherketone with Excellent Antibacterial Properties and Biocompatibility for Implant Abutment. *Macromol. Res.* **2021**, *29*, 351–359.
- (17) Gheysoor, M. XML Study of Biocompatibility and Antibacterial Properties of Titanium Substrates Coated With Chitosan Reinforced With Graphene Oxide. *Iran. J. Med. Microbiol.* **2018**, *12*, 107–115.
- (18) Gurunathan, S.; Han, J. W.; Dayem, A. A.; Eppakayala, V.; Park, M.-R.; Kwon, D.-N.; Kim, J.-H. Antibacterial Activity of Dithiothreitol Reduced Graphene Oxide. *J. Ind. Eng. Chem.* **2013**, *19*, 1280–1288.
- (19) Lu, B.; Li, T.; Zhao, H.; Li, X.; Gao, C.; Zhang, S.; Xie, E. Graphene-Based Composite Materials Beneficial to Wound Healing. *Nanoscale* **2012**, *4*, 2978.
- (20) Li, Q.; Liang, B.; Wang, F.; Wang, Z. Delivery of Interleukin 4 from a Titanium Substrate Coated with Graphene Oxide for Enhanced Osseointegration by Regulating Macrophage Polarization. *ACS Biomater. Sci. Eng.* **2020**, *6*, 5215–5229.
- (21) Han, J.; Kim, Y. S.; Lim, M.-Y.; Kim, H. Y.; Kong, S.; Kang, M.; Choo, Y. W.; Jun, J. H.; Ryu, S.; Jeong, H.-Y.; Park, J.; Jeong, G.-J.; Lee, J.-C.; Eom, G. H.; Ahn, Y.; Kim, B.-S. Dual Roles of Graphene Oxide To Attenuate Inflammation and Elicit Timely Polarization of Macrophage Phenotypes for Cardiac Repair. *ACS Nano* **2018**, *12*, 1959–1977.
- (22) Xue, D.; Chen, E.; Zhong, H.; Zhang, W.; Wang, S.; Joomun, M. U.; Yao, T.; Tan, Y.; Lin, S.; Zheng, Q.; Pan, Z. Immunomodulatory Properties of Graphene Oxide for Osteogenesis and Angiogenesis. *Int. J. Nanomed.* **2018**, *Volume 13*, 5799–5810.
- (23) Han, K.; Bai, Q.; Wu, W.; Sun, N.; Cui, N.; Lu, T. Gelatin-Based Adhesive Hydrogel with Self-Healing, Hemostasis, and Electrical Conductivity. *Int. J. Biol. Macromol.* **2021**, *183*, 2142–2151.
- (24) Tan, J.; Li, Y.; Liu, Z.; Qu, S.; Lu, X.; Wang, J.; Duan, K.; Weng, J.; Feng, B. Anti-Infection Activity of Nanostructured Titanium Percutaneous Implants with a Postoperative Infection Model. *Appl. Surf. Sci.* **2015**, *344*, 119–127.
- (25) Hu, C.; Yang, Y.; Lin, Y.; Wang, L.; Ma, R.; Zhang, Y.; Feng, X.; Wu, J.; Chen, L.; Shao, L. GO-Based Antibacterial Composites: Application and Design Strategies. *Adv. Drug Delivery Rev.* **2021**, *178*, No. 113967.
- (26) Ali, I. H.; Ouf, A.; Elshishiny, F.; Taskin, M. B.; Song, J.; Dong, M.; Chen, M.; Siam, R.; Mamdouh, W. Antimicrobial and Wound-Healing Activities of Graphene-Reinforced Electrospun Chitosan/Gelatin Nanofibrous Nanocomposite Scaffolds. *ACS Omega* **2022**, *7*, 1838–1850.
- (27) Nokoorani, Y. D.; Shamloo, A.; Bahadoran, M.; Moravvej, H. Fabrication and Characterization of Scaffolds Containing Different

Amounts of Allantoin for Skin Tissue Engineering. *Sci. Rep.* **2021**, *11*, No. 16164.

(28) Kanakia, S.; Toussaint, J. D.; Mullick Chowdhury, S.; Tembulkar, T.; Lee, S.; Jiang, Y.-P.; Lin, R. Z.; Shroyer, K. R.; Moore, W.; Sitharaman, B. Dose Ranging, Expanded Acute Toxicity and Safety Pharmacology Studies for Intravenously Administered Functionalized Graphene Nanoparticle Formulations. *Biomaterials* **2014**, *35*, 7022–7031.

(29) Dinescu, S.; Ionita, M.; Pandele, A. M.; Galateanu, B.; Iovu, H.; Ardelean, A.; Costache, M.; Hermenean, A. In Vitro Cytocompatibility Evaluation of Chitosan/Graphene Oxide 3D Scaffold Composites Designed for Bone Tissue Engineering. *Bio-Med. Mater. Eng.* **2014**, *24*, 2249–2256.

(30) Zaveri, T. D.; Lewis, J. S.; Dolgova, N. V.; Clare-Salzler, M. J.; Keselowsky, B. G. Integrin-Directed Modulation of Macrophage Responses to Biomaterials. *Biomaterials* **2014**, *35*, 3504–3515.

(31) Lee, H.-S.; Stachelek, S. J.; Tomczyk, N.; Finley, M. J.; Composto, R. J.; Eckmann, D. M. Correlating Macrophage Morphology and Cytokine Production Resulting from Biomaterial Contact. *J. Biomed. Mater. Res.* **2013**, *101A*, 203–212.

(32) Cicuéndez, M.; Casarrubios, L.; Barroca, N.; Silva, D.; Feito, M. J.; Diez-Orejas, R.; Marques, P. A. A. P.; Portolés, M. T. Benefits in the Macrophage Response Due to Graphene Oxide Reduction by Thermal Treatment. *Int. J. Mol. Sci.* **2021**, *22*, 6701.

(33) Wang, W.; Liu, Y.; Yang, C.; Qi, X.; Li, S.; Liu, C.; Li, X. Mesoporous Bioactive Glass Combined with Graphene Oxide Scaffolds for Bone Repair. *Int. J. Biol. Sci.* **2019**, *15*, 2156–2169.